QUALITY COMPARISON OF DIGITAL AND FILM-BASED IMAGES FOR PHOTOGRAMMETRIC PURPOSES

Roland Perko[1]   **Andreas Klaus**[2]   **Michael Gruber**[3]

[1] Institute for Computer Graphics and Vision, Graz University of Technology, Inffeldgasse 16, 8010 Graz, Austria
email: `perko@icg.tu-graz.ac.at`

[2] VRVis Research Center, Inffeldgasse 16, 8010 Graz, Austria
email: `klaus@vrvis.at`

[3] Vexcel Imaging GmbH, Münzgrabenstraße 11, 8010 Graz, Austria
email: `mgruber@vexcel.co.at`

KEY WORDS: Comparison, Digital, Analog, Sensors, Aerial.

ABSTRACT

Digital cameras are replacing analog film not only on the consumer market. New digital aerial cameras such as Vexcel Imaging UltraCam$_D$ or Z/I DMC implement novel concepts that make the changeover to digital photogrammetry possible. The comparison of image quality of these sensors is important when switching from analog to digital. In this paper we propose algorithms of how to assess image quality, whereas the main focus is set to stereo matching which is the fundamental for several photogrammetric procedures, like generation of digital elevation models or true orthophotos. We use test image data from an experimental setup. We took images with a 11 megapixel CCD sensor and analog small format camera with several types of film. The focal lengths of the used lenses are chosen in that way, that a $9\mu m$ digital pixel (native CCD pixel size) represents the same object point as a pixel from a $20\mu m$ film scan. With this constellation we are able to show that the quality of a $9\mu m$ CCD pixels outperforms the quality of a $20\mu m$ or less scanned film pixel. The main disadvantage of analog film is its granularity that causes grain noise. To measure the impacts of grain noise to image processing tasks, we use the following algorithms on artificial and natural images: Distances to the epipolar ray of stereo matching results, Blonksi and Luxen edge response test, minimal radius of Siemens star and noise measurement via entropy. In contrast to film images that feature a dynamic range of 8 bit, images captured with digital sensors feature a high dynamic range of 12 bit and contain almost no noise. This makes the matching of poorly textured structures in digitally sensed images possible with high accuracy, even when the matching in conventional film images fails. Stereo matching on digital images results in a 2.5 times smaller noise level. The conclusion of the proposed work is that digital sensors are leading to highly accurate and robust photogrammetric processing.

1 INTRODUCTION

New digital aerial cameras such as Vexcel Imaging Ultra-Cam$_D$ (Leberl et al., 2003) or Z/I DMC (Hinz et al., 2000) implement novel concepts that make the changeover to digital photogrammetry possible. In our previous work we compared film-based images scanned with $15\mu m$ with digital sensed images (Perko and Gruber, 2002). Now we compare images taken from camera UltraCam$_D$ with film-based images scanned at 5, 10, 15 and $20\mu m$. The focal lengths of the used lenses are chosen in that way, that a $9\mu m$ digital pixel represents the same object point as a pixel from a $20\mu m$ film scan.

For digital sensing we are using the camera UltraCam$_D$ with $100mm/f : 5.6$ *apo digitar* lens and 11 megapixels CCD sensor Dalsa TFT4027 with $9\mu m$ pixelsize which gives 12 bit radiometric resolution (denoted as ccd in the rest of this paper). To match the requirements that a film pixel scanned at $20\mu m$ equals a ccd pixel of $9\mu m$ the focal length of the analog camera should be $f_{film} = \frac{20\mu m}{9\mu m} f_{ccd} = 222.2mm$.

Analog small format film images are taken using camera *Minolta Dynax 7* with *Sigma 135-400mm/f1:4.5-5.6* lens fixed at $222mm$ and then scanned with high precision scan-

ner *UltraScan 5000* (Vexcel Imaging Austria, 2002) at 5, 10, 15 and $20\mu m$ at dynamic range of 16 bit. Four small format films Agfa APX 100 (Agfa, 2003), Ilford Delta 100 (Ilford, 2002), Kodak T-MAX (Kodak, 2002, Kodak, 2004) and Kodak T-PAN (Kodak, 2003) were used (denoted as apx, delta, t-max and t-pan in the rest of this paper). Both cameras are geometrically calibrated with high accuracy.

The paper is structured as follows. First, we propose algorithms of how to assess image quality (section 2). Next, results are given in section 3. Finally, concluding remarks are made in section 4.

2 TESTING METHODS

We propose three tests to evaluate the geometric accuracy of images, namely image matching, edge response and Siemens star test and one test for noise measurement.

2.1 Image matching

To evaluate the geometric accuracy of images, we propose a stereo image matching setup. Homologous points of two images taken from the same device from different spots

are taken. Via epipolar geometry the distance from every point to the according epipolar line is taken as a quality measure for image matching. Image matching is done by extracting points of interest using Harris operator (Harris and Stephens, 1988) and trying to reallocate them by area based matching using normalized cross correlation as similarity measure. We normalize the cross correlation to get correlation coefficients using the definition of (Haralick and Shapiro, 1992) generalized to two-dimensions. For refining the results to subpixel accuracy a least squares approach is used which fits a paraboloid into the correlation coefficient matrix (Gleason et al., 1990). Then the epipolar geometry is estimated based on MAPSAC algorithm (Torr, 2002a) which is implemented within a free Matlab toolbox (Torr, 2002b). The MAPSAC algorithm is an extension of standard eight point algorithms (Zhang, 1997).

2.2 Edge response

The quality of an imaging system may be evaluated using the amount of blurring at edges. The edge spread function of a 1D signal is the response of the system to an ideal edge. The first derivative of the edge spread function, called the point spread function (PSF), is usually used to describe the quality of an imaging system (Luxen and Förstner, 2002).

We choose two different measures to characterize the edge response function.

Blonski edge response
The modern measurement of geometric resolution is the edge response. The transition from bright to dark defines the edge sharpness and is considered to be a measure of geometric resolution. Every ideal step edge is blurred when captured with an imaging device (see figure 1). This blurring describes a measure for the optical system. (Blonski et al., 2002) suggest to fit a sigmoid function $f(x) = \frac{1}{1+e^{-ax}}$ into the edge profile and characterize spatial resolution by full width at half maximum of the first derivative of this sigmoid edge signal (see figure 2). This first derivative is called a line spread function and its full width (measured in pixels) at 50% of maximum amplitude characterizes the whole imaging process.
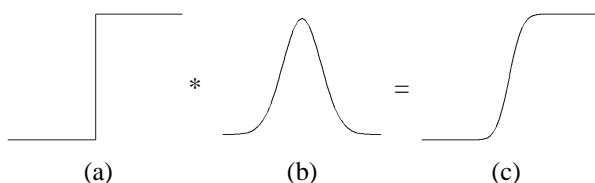

Figure 1: Edge response: Ideal step edge (a) is corrupted by blurring, noise or other distortions (b) which leads to a loss of edge sharpness (c).

Luxen edge response
The basic idea of (Luxen and Förstner, 2002) is to measure the PSF by calculating the edge direction and edge magnitude of a sensed image. Then the magnitudes get plotted
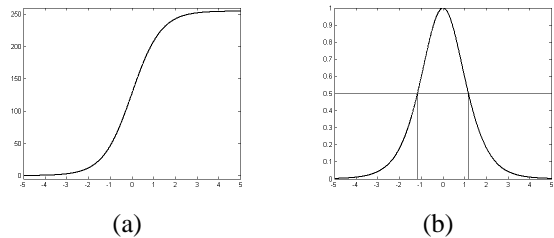

Figure 2: Edge response: (a) Fitted sigmoid function into the edge profile and (b) first derivative of (a) with marked full width at half maximum.

according to the edge directions and the surrounding ellipse describes the parameters of the PSF. This process is very sensitive to noise, so we are not using the surrounding but a fitted ellipse in the least squares sense. The width of the ellipse is normalized within the interval $[0, 1]$ where a width of 1 stands for an ideal edge. The width of the ellipse is increasing in size reciprocally quadratic with image sharpness. This relation is important for comparison of different image resolutions. For calculating the first derivative optimally rotation-equivariant directional derivative kernels by (Farid and Simoncelli, 1997) are used. Figure 3 shows the calculated magnitude image of an Siemens star and the plotted edges according to their directions.
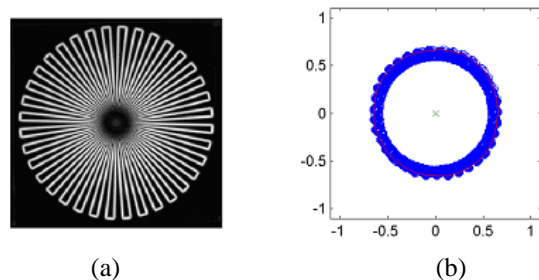

Figure 3: Luxen edge response test: (a) Edge magnitude of a Siemens star image (b) magnitude plotted according to edge direction with ellipse fitted in the least squares sense.

2.3 Siemens star test

A Siemens star is a special bar-pattern containing a very wide range of spatial frequencies. The Siemens star consists of an even number of tapered wedges pointing to a common center. Along each concentric circle centered on the star a rectangular signal may be achieved. For smaller radii the signal frequency is increasing until it reaches the limiting spatial frequency. The limited spatial frequency where all edges of the Siemens star could be detected is a measurement of image quality and is described by the minimal radius in pixels. Figure 4 shows a Siemens star and the according bar patterns for different radii.

2.4 Noise estimation via entropy

Noise is an important criterion for measuring image quality. In our test data, noise in the scanned film images is mainly caused by the granularity of the film. To measure noise the entropy H_e is calculated in homogenous patches
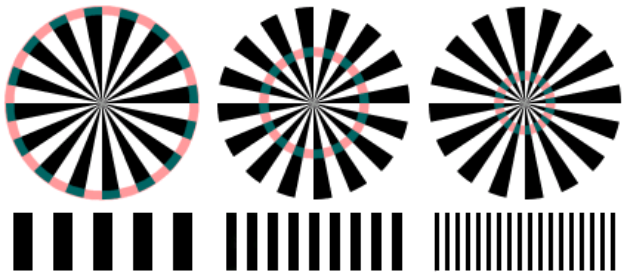
Figure 4: Siemens star with 32 wedges: For smaller radii the spatial frequency of concentric circles is increasing. The smallest radius where all wedges are resolved characterizes the quality of the image.

of the test images,

$$H_e = -\sum_{k=0}^{G-1} P(k) log_2[P(k)]$$

for an image with G gray-levels and the probability of gray-level k is $P(k)$. For an ideal homogenous patch containing only one gray-level the entropy is 0. Smaller entropy indicates less information content and is a measure for image noise, if calculated in a homogenous patch.

3 RESULTS

All testing methods were performed on all film images scanned with 5, 10, 15 and $20\mu m$ and on the ccd images with $9\mu m$ which covers the same area as the $20\mu m$ scans. If we have an ideal film image and an ideal scanner we could scan the image with e.g. double resolution and will get the same results for e.g. the Siemens star test. As we are dealing with real film images it is obvious that the geometric performance will not stay the same when scanning with very high resolution, because the granularity of the film causes image noise.

In the following tables the values in brackets are the ratios to the $5\mu m$ scans. If the ratio is higher than the ratio between the resolutions (i.e. between $5\mu m$ and $15\mu m$ we have ratio of 3), this indicates that there is no more information in the $5\mu m$ image than in the lower resolution one. So if the ratio is about 2.0 for the $10\mu m$, 3.0 for the $15\mu m$ and 4.0 for the $20\mu m$ scan, then we know that the $20\mu m$ scan contains same geometric accuracy as the $5\mu m$ and therefore scanning with $20\mu m$ makes sense without losing information.

For ideal images the ratio is 1.0 independent of the resolution.

3.1 Image matching

For the image matching setup we used stereo images with a baseline of about 10 meters. One of the stereo images is shown in figure 5. Then 10000 points of interest were extracted from the reference image and reallocated in the search image. Reference and search window size were adapted according to the scan size. For example if we have a search window size of 600×80 pixel in the $5\mu m$ case, then the window size for the $20\mu m$ case is smaller by a

factor of 4, so 150×20 pixels. This guarantees that these windows covers the same area in the real object.

Figure 5: One image of the stereo scene taken with ccd sensor. Shown are 1800×1200 pixels.

Figure 6 shows the histograms of the absolute distances to the epipolar lines for film *delta* scanned with 5, 10, 15 and $20\mu m$. The histograms are scaled so that each histogram shows the same distances in object space (e.g. 8 pixels in $5\mu m$ are 2 pixels in a $20\mu m$ scan). As quality measure we choose full width at half maximum, called σ. The ratios of these σ values are 2.06, 2.91 and 3.12 which means that the $15\mu m$ scan leads to same accuracy as the $5\mu m$ scan, but scanning with $20\mu m$ leads to a slight loss of quality. All results for this test are given in table 1.

Figure 7 shows the histograms for $20\mu m$ scans and for the ccd image. The number of matched points is significantly higher for ccd case and the σ value of ccd outperforms the film with a factor of 2 to 3, which means on average 2.5 times better image matching results.

Table 2 shows the maximal absolute distance for the best 1000 matches and here the accuracy in $20\mu m$ scan is even better than using the $5\mu m$ scan. The digital ccd image outperforms the $20\mu m$ scans by a factor of 3.0 to 5.0.

	$5\mu m$	$10\mu m$	$15\mu m$	$20\mu m$
apx	2.078	1.156 (1.80)	0.724 (2.87)	0.656 (3.17)
delta	2.000	0.969 (2.06)	0.688 (2.91)	0.641 (3.12)
t-max	1.950	0.924 (2.11)	0.691 (2.82)	0.453 (4.30)
t-pan	1.989	1.042 (1.91)	0.732 (2.71)	0.453 (4.39)
ccd $9\mu m$	-	-	-	0.219

Table 1: Full width at half height of distances to the epipolar line in pixels (values in the brackets are the ratios to $5\mu m$ scan).

	$5\mu m$	$10\mu m$	$15\mu m$	$20\mu m$
apx	1.232	0.597 (2.06)	0.386 (3.19)	0.272 (4.53)
delta	1.080	0.397 (2.72)	0.288 (3.75)	0.229 (4.72)
t-max	0.739	0.278 (2.66)	0.226 (3.14)	0.183 (4.04)
t-pan	0.803	0.315 (2.55)	0.268 (3.00)	0.171 (4.70)
ccd $9\mu m$	-	-	-	0.0557

Table 2: Maximal distances to the epipolar of the 1000 best matches in pixels (values in the brackets are the ratios to $5\mu m$ scan).
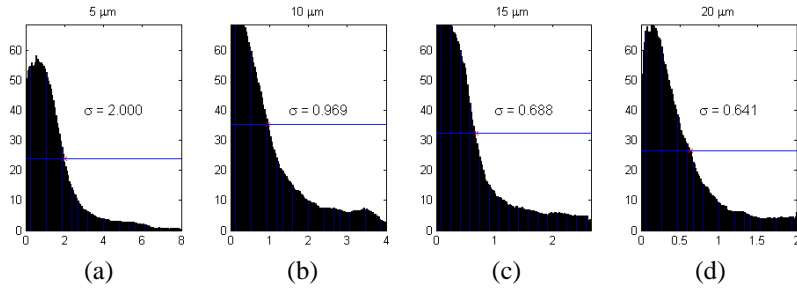
Figure 6: Distance to epipolar line in pixels for film *delta* scanned with (a) $5\mu m$ (b) $10\mu m$ (c) $15\mu m$ and (d) $20\mu m$.
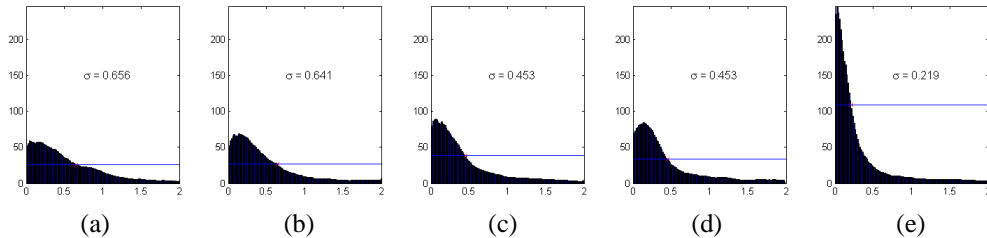

Figure 7: Distance to epipolar line in pixels for films (a) apx (b) delta (c) t-max and (d) t-pan scanned with $20\mu m$ and (e) ccd with $9\mu m$.

3.2 Edge response

Table 3 gives the results for the Blonski edge response test. The width of edges is shown in pixels and again the $20\mu m$ leads even to better results than using the $5\mu m$ images. Here the ccd is comparable to $20\mu m$ scan. The Luxen test (see table 4) behaves the same.

	$5\mu m$	$10\mu m$	$15\mu m$	$20\mu m$
apx	5.743	2.167 (2.65)	1.451 (3.96)	1.117 (5.14)
delta	5.222	2.034 (2.57)	1.586 (3.29)	1.115 (4.68)
t-max	5.621	2.310 (2.43)	1.496 (3.76)	1.138 (4.94)
t-pan	5.426	2.141 (2.53)	1.421 (3.82)	1.104 (4.91)
ccd $9\mu m$	-	-	-	1.111

Table 3: Width of edges for Blonski edge response test in pixels (values in the brackets are the ratios to $5\mu m$ scan).

	$5\mu m$	$10\mu m$	$15\mu m$	$20\mu m$
apx	0.266	0.424 (2.54)	0.529 (3.96)	0.601 (5.10)
delta	0.253	0.418 (2.73)	0.530 (4.39)	0.595 (5.53)
t-max	0.261	0.418 (2.56)	0.518 (3.94)	0.580 (4.94)
t-pan	0.247	0.414 (2.81)	0.536 (4.71)	0.613 (6.16)
ccd $9\mu m$	-	-	-	0.623

Table 4: Width of edge magnitude ellipse from Luxen test normalized to the interval $[0, 1]$ (values in the brackets are the squared ratios to $5\mu m$ scan).

3.3 Siemens star test

In this test we used a Siemens star test target with 72 wedges. The minimal possible radius according to the Kell factor is given with $r_{min} = \frac{72}{2*\pi}\sqrt{2} \approx 16$. Again the $20\mu m$ scan gives same results as the $5\mu m$ one and ccd performs equivalent.

3.4 Noise estimation via entropy

Noise is measured using two homogenous image patches. The one within a bright area (table 6) and the other one within a dark area (table 7). In this test the ccd image is

	$5\mu m$	$10\mu m$	$15\mu m$	$20\mu m$
apx	64	33 (1.94)	22 (2.91)	16 (4.00)
delta	66	32 (2.06)	19 (3.47)	16 (4.13)
t-max	65	35 (1.86)	21 (3.10)	16 (4.06)
t-pan	63	36 (1.75)	22 (2.86)	18 (3.50)
ccd $9\mu m$	-	-	-	16

Table 5: Minimal resolving radius for the Siemens star test in pixels (values in the brackets are the ratios to $5\mu m$ scan).

radiometrically scaled to 16 Bit to make the results comparable. Noise in the digital sensed image is significantly lower in comparison to the analog one and this is also the main reason why the geometrically test yields better results for the ccd images.

	$5\mu m$	$10\mu m$	$15\mu m$	$20\mu m$
apx	11.551	11.539	11.332	11.160
delta	11.968	11.962	11.869	11.778
t-max	12.201	12.166	12.052	11.954
t-pan	12.462	12.415	12.310	12.217
CCD $9\mu m$	-	-	-	7.608

Table 6: Entropy within a bright homogenous image patch in Bits.

	$5\mu m$	$10\mu m$	$15\mu m$	$20\mu m$
apx	12.916	12.203	11.422	10.759
delta	12.797	12.185	11.426	10.765
t-max	12.709	12.049	11.305	10.709
t-pan	11.773	11.360	10.832	10.337
CCD $9\mu m$	-	-	-	8.599

Table 7: Entropy within a dark homogenous image patch in Bits.

4 CONCLUSION

We have compared film-based images scanned with 5, 10, 15 and $20\mu m$ and ccd-based images. In general all four used films perform quite similar whereas the Kodak T-PAN and Kodak T-MAX are a little bit better in comparison to

the Afga and Ilford films. First, taking into account the different resolutions as a factor between the test results, the information and quality of the analog images scanned at the different resolutions are quite similar. The conclusion is that scanning a film image with $5\mu m$ is unnecessary because the $20\mu m$ scan contains the same information. There is no more information included in the film and thus cannot be revealed by scanning at higher resolution. Second, the digital sensed images are equal to the $20\mu m$ scanned film image in the edge response and Siemens star tests, but outperforms the film images in stereo matching accuracy. Stereo matching results in a 2.5 times smaller noise level and it is possible to match also in poorly textured ares because of the absence of noise.

The conclusion of the work is that digital sensors are leading to highly accurate and robust photogrammetric processing. The next stage is to perform these tests on synchronized exposed aerial images of digital UltraCam$_D$ and analog RMK Top from an airplane holding both cameras on the same flight.

REFERENCES

Agfa, 2003. Agfa Technical Data - Agfa Professional Films. Report F-PF-E4, 4th Edition.

Blonski, S., Pagnutti, M., Ryan, R. E. and Zanoni, V., 2002. In-flight edge response measurements for high-spatial-resolution remote sensing systems. In: W. L. Barnes (ed.), Proceedings of SPIE: Earth Observing Systems VII, Vol. 4814, pp. 317–326.

Farid, H. and Simoncelli, E. P., 1997. Optimally rotation-equivariant directional derivative kernels. In: Computer Analysis of Images and Patterns, pp. 207–214.

Gleason, S. S., Hunt, M. A. and Jatko, W. B., 1990. Sub-pixel measurement of image features based on paraboloid surface fit. Proc. Machine Vision Systems Integration in Industry, SPIE, Boston MA.

Haralick, R. M. and Shapiro, L. G., 1992. Computer and Robot Vision. Vol. 2, Addison-Wesley Publishing Company.

Harris, C. and Stephens, M., 1988. A combined corner and edge detector. Proceedings 4th Alvey Visual Conference pp. 189–192.

Hinz, A., Dörstl, C. and Heier, H., 2000. Digital modular camera: System concept and data processing workflow. Archives of the Intl. Soc. for photogrammetry and remote sensing. Amsterdam, The Netherlands.

Ilford, 2002. Ilford 100 Delta Professional. Report No. 95026A.www.

Kodak, 2002. KODAK Technical Data - T-MAX Professional Films. KODAK Publication No. F-32, CAT 155 8527.

Kodak, 2003. KODAK Technical Data - Professional Technical Pan Film. KODAK Publication No. P-255, CAT 817 2785.

Kodak, 2004. KODAK Technical Data - T-MAX Professional Films. KODAK Publication No. F-4016.

Leberl, F., Gruber, M., Ponticelli, M., Bernoegger, S. and Perko, R., 2003. The UltraCam large format aerial digital camera system. Proceedings of the American Society for Photogrammetry & Remote Sensing, Anchorage, Alaska.

Luxen, M. and Förstner, W., 2002. Characterizing image quality: Blind estimation of the point spread function from a single image. ISPRS Commission III: Theory and Algorithms XXXIV(3A), pp. 205–210.

Perko, R. and Gruber, M., 2002. Comparison of quality and information content of digital and film-based images. ISPRS Commission III: Theory and Algorithms XXXIV(3B), pp. 206–209.

Torr, P. H. S., 2002a. Bayesian model estimation and selection for epipolar geometry and generic manifold fitting. International Journal of Computer Vision 50(1), pp. 35–61.

Torr, P. H. S., 2002b. A structure and motion toolkit in matlab: Interactive adventures in s and m. Technical Report MSR-TR-2002-56, Microsoft Research.

Vexcel Imaging Austria, 2002. Ultrascan 5000 - Precision photogrammetric scanning. VIA001PB-1002 rev 0.1.

Zhang, Z., 1997. Determining the epipolar geometry and its uncertainty: A review. International Journal of Computer Vision 27(2), pp. 161–195.